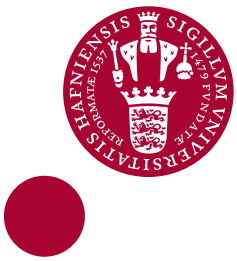

ALICE results on system-size dependence of charged-particle multiplicity density in p-Pb, Pb-Pb and Xe-Xe collisions

Alice Collaboration

Published in:
Nuclear Physics A

DOI:
10.1016/j.nuclphysa.2018.09.060

Publication date:
2019

Document version
Publisher's PDF, also known as Version of record

Available online at www.sciencedirect.com

ScienceDirect

Nuclear Physics A 982 (2019) 279–282

NUCLEAR PHYSICS A

www.elsevier.com/locate/nuclphysa

XXVIIth International Conference on Ultrarelativistic Nucleus-Nucleus Collisions (Quark Matter 2018)

ALICE results on system-size dependence of charged-particle multiplicity density in p–Pb, Pb–Pb and Xe–Xe collisions

Beomkyu Kim
(for the ALICE Collaboration)

INHA University, 100 Inha-ro, Michuhol-gu, Incheon 22212, KOREA

Abstract

Particle production at LHC energies involves the interplay of hard (perturbative) and soft (non-perturbative) QCD processes. Global observables, such as the charged-particle multiplicity, are related to the initial geometry and the energy density produced in the collision. They are important to characterise relativistic heavy-ion collisions and to constrain model calculations. The LHC produced Xenon–Xenon collisions for the first time in October 2017. New results on the primary charged-particle pseudorapidity density, and its pseudorapidity and centrality dependence are presented for this lighter and deformed nucleus, and compared to measurements obtained for lead ions. New results will also be presented for p-Pb collisions at the highest energy of 8.16 TeV, as part of an overview of all the measurements at LHC Run 1 and 2 energies. These studies allow us to investigate the evolution of particle production with energy and system size and to compare models based on various particle production mechanisms and different initial conditions.

Keywords:
ALICE, LHC, Xe–Xe, Pb–Pb, p–Pb, pp, Charged-particle multiplicity density, System-size dependence

1. Introduction

For the last 8 years from 2010 to 2018, the ALICE Collaboration has provided results of primary-charged-particle production in various collision energies and systems. In October 2017, LHC collided xenon ions at $\sqrt{s_{\rm NN}}$ = 5.44 TeV. Central collisions of heavy ions, like Pb (atomic number A = 208) revealed Quark-Gluon Plasma (QGP) effects. Xe has fewer nucleons (A = 129) than Pb and is a good medium-sized ion to check how the system size of a colliding system relates to the creation of the hot and dense medium. On the other hand, QGP-like effects have been observed even in pp and p–A collisions, the so-called small systems [1, 2, 3]. In high multiplicity pp and p–Pb collisions, the process of the Multi Parton Interactions (MPI) [4] becomes more important and is supposed to be related to QGP-like effect [5]. Particle production at few GeV/c is dominated by soft QCD and makes a big contribution to the charged-particle multiplicity density. This can be approached by phenomenological modelling.

https://doi.org/10.1016/j.nuclphysa.2018.09.060
0375-9474/

2. Analysis method

Primary charged-particle multiplicity density, $\mathrm{d}N_{\mathrm{ch}}/\mathrm{d}\eta$, is measured by counting the number of tracklets (a short track segment) using the SPD detector [6] in the central region ($-1.8 < \eta < 1.8$) and estimating the effective energy density per charged particle using the FMD detector [7, 8] in the forward regions ($-3.5 < \eta < -1.8$ and $1.8 < \eta < 5$). Data were collected with a minimum bias trigger requiring a coincidence of signals in each side of V0 sub-detectors (V0A and V0C) [9, 8]. The primary interaction vertex of a collision is obtained by extending correlated hits in the two silicon-pixel layers of the SPD to the beam pipe of the LHC. Centrality estimation is based on a Glauber approach [10, 11] by fitting to the V0 amplitude distribution [12] for the Pb-going side (V0A) in p–Pb collisions or for both A-going sides (V0A and V0C) in Pb–Pb and Xe–Xe collisions. The amplitude of the V0 detector is fitted with a two-component model given by $N_{\mathrm{sources}} = f \times N_{\mathrm{part}} + (1-f) \times N_{\mathrm{coll}}$ where f fixes the relative contributions of N_{part} (the number of participating nucleons taking part in the collision) and N_{coll} (the number of binary collisions among participating nucleons), and N_{sources} is the number of intermediate sources for the particle production to be transformed to the charged-particle multiplicity by the negative binomial distribution (NBD). The detailed systematic studies in p–Pb, Pb–Pb and Xe–Xe collisions can be found elsewhere [13, 14, 15, 16].

3. Results and discussion

Figure 1a shows $\mathrm{d}N_{\mathrm{ch}}/\mathrm{d}\eta$ in p–Pb collisions at $\sqrt{s_{\mathrm{NN}}} = 8.16$ TeV and the result is compared with theoretical models. Phenomenological models like HIJING [17, 18], EPOS LHC [19] and EPOS 3 [20] reproduce the data better for the Pb-going side than for the proton-going side. Saturation-based models like rc-BK [21, 22] and KLN [23] describe the data better in $\eta_{\mathrm{lab}} > -1.3$ as expected. However, all models describe the data within ±15%. The $\mathrm{d}N_{\mathrm{ch}}/\mathrm{d}\eta$ for the top 5% central Xe–Xe collisions is shown and compared to models in Fig. 1b. The pseudorapidity dependence of $\mathrm{d}N_{\mathrm{ch}}/\mathrm{d}\eta$ is described by the models within ±10% in $|\eta| < 4$ except for EPOS LHC.

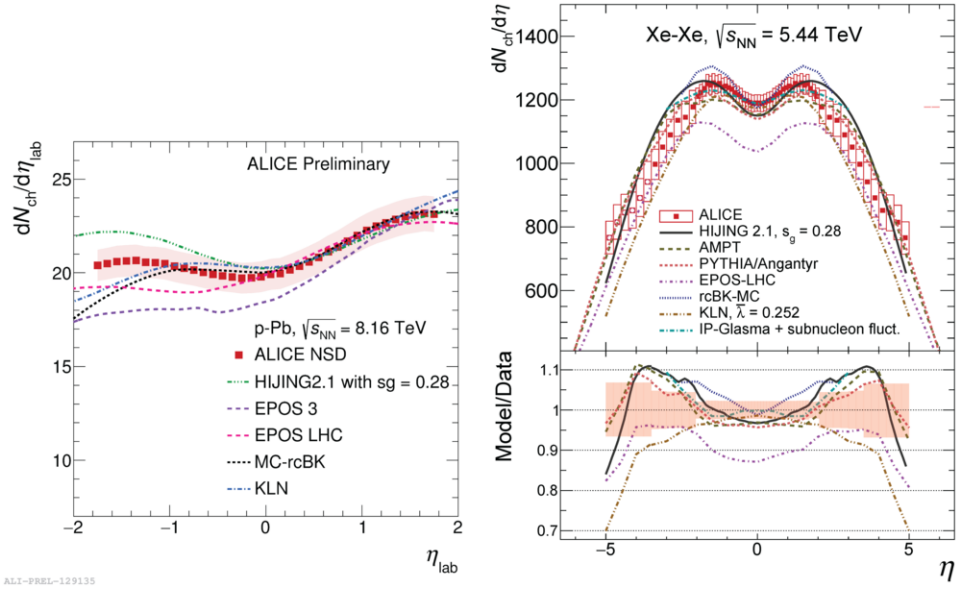

(a) $\mathrm{d}N_{\mathrm{ch}}/\mathrm{d}\eta$ in p–Pb collisions

(b) $\mathrm{d}N_{\mathrm{ch}}/\mathrm{d}\eta$ for the top 5% central Xe–Xe collisions [13]

Figure 2a shows $\frac{2}{\langle N_{\mathrm{part}} \rangle} \langle \mathrm{d}N_{\mathrm{ch}}/\mathrm{d}\eta \rangle$ for the top 5% central Xe–Xe collisions compared to previous measurements for AA collisions as a function of $\sqrt{s_{\mathrm{NN}}}$, as well as for inelastic and Non-Single Diffractive (NSD)

pp, p$\bar{\text{p}}$ and NSD pA and dA collisions. The lines are power law fits to the data. For the 0–5% central AA collisions, the Xe–Xe result fits with the power-law trend previously established by the various measurements. It indicates that Xe still acts like a heavy ion compared to the pp and pA trends that are far from the central AA collisions. The results in pA collisions for NSD are overlaid with the pp and p$\bar{\text{p}}$ trend of INEL collisions. This can be interpreted as if the contribution from diffractive processes is negligible in pA collisions. Figure 2b shows $\frac{2}{\langle N_{\text{part}}\rangle}\langle \text{d}N_{\text{ch}}/\text{d}\eta\rangle$ in $|\eta| < 0.5$ as a function of $\langle N_{\text{part}}\rangle$ for various collision systems and collision energies. The distributions of Xe–Xe at $\sqrt{s_{\text{NN}}}$ = 5.44 TeV and Pb–Pb at $\sqrt{s_{\text{NN}}}$ = 5.02 TeV decrease by a factor of 2 from the most central to peripheral collisions and smoothly connect to the results in pp and p–Pb collisions. A steep rise of the distribution starting from $\langle N_{\text{part}}\rangle$ = 200 for Xe-Xe collisions is newly observed and is thought to result from multiplicity fluctuations due to the smaller size of Xe nucleus than heavier ones like Pb or Au. This can be supported from the trend for Cu–Cu collisions in Fig 2b. The $\langle N_{\text{part}}\rangle$-dependence of $\frac{2}{\langle N_{\text{part}}\rangle}\langle \text{d}N_{\text{ch}}/\text{d}\eta\rangle$ for Xe–Xe collisions is also compared with theoretical models in Fig 2c. All the models describe the data within ±20%.

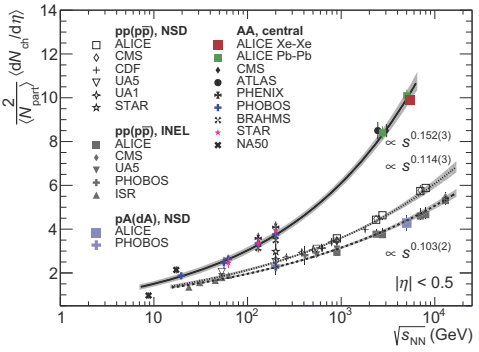

(a) $\frac{2}{\langle N_{\text{part}}\rangle}\langle \text{d}N_{\text{ch}}/\text{d}\eta\rangle$ vs $\sqrt{s}$, $\sqrt{s_{\text{NN}}}$ [13]

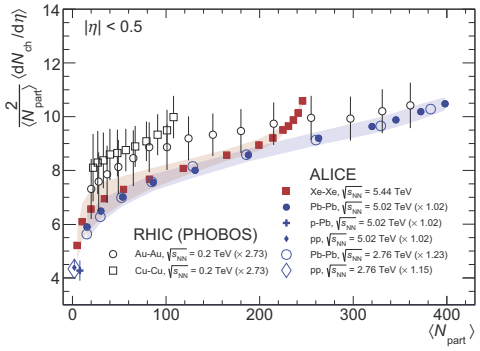

(b) The $\frac{2}{\langle N_{\text{part}}\rangle}\langle \text{d}N_{\text{ch}}/\text{d}\eta\rangle$ vs $\langle N_{\text{part}}\rangle$ [13]

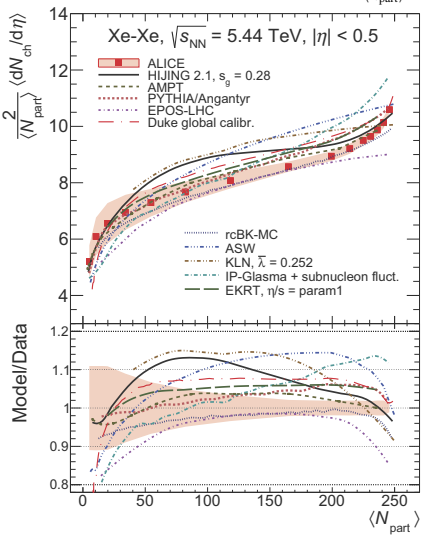

(c) The $\frac{2}{\langle N_{\text{part}}\rangle}\langle \text{d}N_{\text{ch}}/\text{d}\eta\rangle$ vs $\langle N_{\text{part}}\rangle$ in Xe–Xe collisions [13]

Fig. 2: $\frac{2}{\langle N_{\text{part}}\rangle}\langle \text{d}N_{\text{ch}}/\text{d}\eta\rangle$ in AA and pA collisions.

4. Conclusions

An overview of results for charged-particle multiplicity density in LHC Run 1 and 2 energies measured by ALICE in p-Pb, Pb-Pb and Xe-Xe collisions is provided in this proceedings. Newly measured $\mathrm{d}N_{\mathrm{ch}}/\mathrm{d}\eta$ in Xe–Xe collisions at $\sqrt{s_{\mathrm{NN}}}$ = 5.44 TeV shows still a heavy-ion like behaviour. All theoretical models based on various particle production mechanisms and different initial conditions describe $\mathrm{d}N_{\mathrm{ch}}/\mathrm{d}\eta$ vs η and $\frac{2}{\langle N_{\mathrm{part}}\rangle}\langle \mathrm{d}N_{\mathrm{ch}}/\mathrm{d}\eta\rangle$ vs $\langle N_{\mathrm{part}}\rangle$ within ±20% in pA and AA collisions. This study might provide further constraints on models and help to improve our understanding of the evolution of particle production with energy and system size.

References

[1] B. Abelev, et al., Long-range angular correlations on the near and away side in p-Pb collisions at $\sqrt{s_{\mathrm{NN}}}$ = 5.02 TeV, Phys. Lett. B 719 (2013) 29–41. arXiv:1212.2001, doi:10.1016/j.physletb.2013.01.012.

[2] G. Aad, et al., Observation of Associated Near-Side and Away-Side Long-Range Correlations in $\sqrt{s_{\mathrm{NN}}}$ = 5.02 TeV Proton-Lead Collisions with the ATLAS Detector, Phys. Rev. Lett. 110 (18) (2013) 182302. arXiv:1212.5198, doi:10.1103/PhysRevLett.110.182302.

[3] V. Khachatryan, et al., Measurement of long-range near-side two-particle angular correlations in pp collisions at $\sqrt{s}$ =13 TeV, Phys. Rev. Lett. 116 (17) (2016) 172302. arXiv:1510.03068, doi:10.1103/PhysRevLett.116.172302.

[4] T. Sjostrand, M. van Zijl, A Multiple Interaction Model for the Event Structure in Hadron Collisions, Phys. Rev. D 36 (1987) 2019. doi:10.1103/PhysRevD.36.2019.

[5] A. Ortiz, P. Christiansen, E. Cuautle, I. Maldonado, G. Paic, Color reconnection and flow-like patterns in pp collisions, Phys. Rev. Lett. 111 (4) (2013) 042001. arXiv:1303.6326, doi:10.1103/PhysRevLett.111.042001.

[6] R. Santoro, et al., The ALICE Silicon Pixel Detector: Readiness for the first proton beam, JINST 4 (2009) P03023. doi:10.1088/1748-0221/4/03/P03023.

[7] C. H. Christensen, J. J. Gaardhoje, K. Gulbrandsen, B. S. Nielsen, C. Sogaard, The ALICE Forward Multiplicity Detector, Int. J. Mod. Phys. E 16 (2007) 2432–2437. arXiv:0712.1117, doi:10.1142/S0218301307008057.

[8] P. Cortese, et al., ALICE forward detectors: FMD, TO and VO: Technical Design Report, Technical Design Report ALICE, CERN, Geneva, 2004, submitted on 10 Sep 2004.
URL `https://cds.cern.ch/record/781854`

[9] E. Abbas, et al., Performance of the ALICE VZERO system, JINST 8 (2013) P10016. arXiv:1306.3130, doi:10.1088/1748-0221/8/10/P10016.

[10] B. Alver, M. Baker, C. Loizides, P. Steinberg, The PHOBOS Glauber Monte CarloarXiv:0805.4411.

[11] C. Loizides, J. Nagle, P. Steinberg, Improved version of the PHOBOS Glauber Monte Carlo, SoftwareX 1-2 (2015) 13–18. arXiv:1408.2549, doi:10.1016/j.softx.2015.05.001.

[12] B. Abelev, et al., Centrality determination of Pb-Pb collisions at $\sqrt{s_{\mathrm{NN}}}$ = 2.76 TeV with ALICE, Phys. Rev. C 88 (4) (2013) 044909. arXiv:1301.4361, doi:10.1103/PhysRevC.88.044909.

[13] S. Acharya, et al., Centrality and pseudorapidity dependence of the charged-particle multiplicity density in Xe-Xe collisions at $\sqrt{s_{\mathrm{NN}}}$ = 5.44 TeVarXiv:1805.04432.

[14] J. Adam, et al., Centrality dependence of particle production in p-Pb collisions at $\sqrt{s_{\mathrm{NN}}}$= 5.02 TeV, Phys. Rev. C 91 (6) (2015) 064905. arXiv:1412.6828, doi:10.1103/PhysRevC.91.064905.

[15] K. Aamodt, et al., Centrality dependence of the charged–particle multiplicity density at mid–rapidity in Pb–Pb collisions at $\sqrt{s_{\mathrm{NN}}}$ = 2.76 TeV, Phys. Rev. Lett. 106 (2011) 032301. arXiv:1012.1657, doi:10.1103/PhysRevLett.106.032301.

[16] J. Adam, et al., Centrality dependence of the charged-particle multiplicity density at midrapidity in Pb-Pb collisions at $\sqrt{s_{\mathrm{NN}}}$ = 5.02 TeV, Phys. Rev. Lett. 116 (2016) 222302. arXiv:1512.06104, doi:10.1103/PhysRevLett.116.222302.

[17] R. Xu, W.-T. Deng, X.-N. Wang, Nuclear modification of high-pT hadron spectra in p+A collisions at LHC, Phys. Rev. C 86 (2012) 051901. arXiv:1204.1998, doi:10.1103/PhysRevC.86.051901.

[18] W.-T. Deng, X.-N. Wang, R. Xu, Hadron production in p+p, p+Pb, and Pb+Pb collisions with the HIJING 2.0 model at energies available at the CERN Large Hadron Collider, Phys. Rev. C 83 (2011) 014915. arXiv:1008.1841, doi:10.1103/PhysRevC.83.014915.

[19] T. Pierog, I. Karpenko, J. M. Katzy, E. Yatsenko, K. Werner, EPOS LHC: Test of collective hadronization with data measured at the CERN Large Hadron Collider, Phys. Rev. C 92 (3) (2015) 034906. arXiv:1306.0121, doi:10.1103/PhysRevC.92.034906.

[20] S. Porteboeuf, T. Pierog, K. Werner, Producing Hard Processes Regarding the Complete Event: The EPOS Event Generator, in: Proceedings, 45th Rencontres de Moriond on QCD and High Energy Interactions: La Thuile, Italy, March 13-20, 2010, Gioi Publishers, Gioi Publishers, 2010, pp. 135–140. arXiv:1006.2967.
URL `https://inspirehep.net/record/858343/files/arXiv:1006.2967.pdf`

[21] J. L. Albacete, A. Dumitru, H. Fujii, Y. Nara, CGC predictions for p + Pb collisions at the LHC, Nucl. Phys. A 897 (2013) 1–27. arXiv:1209.2001, doi:10.1016/j.nuclphysa.2012.09.012.

[22] J. L. Albacete, A. Dumitru, A model for gluon production in heavy-ion collisions at the LHC with rcBK unintegrated gluon densitiesarXiv:1011.5161.

[23] A. Dumitru, D. E. Kharzeev, E. M. Levin, Y. Nara, Gluon Saturation in pA Collisions at the LHC: KLN Model Predictions For Hadron Multiplicities, Phys. Rev. C 85 (2012) 044920. arXiv:1111.3031, doi:10.1103/PhysRevC.85.044920.